Modifications for *ab initio* calculations of the moderately large-embedded-cluster model. Hydrogen adsorption on a lithium surface

Yoshifumi Fukunishi
Department of Synthetic Chemistry, Faculty of Engineering, Kyoto University, Sakyou-ku, 606 Kyoto, Japan

Hiroshi Nakatsuji
Department of Synthetic Chemistry, Faculty of Engineering, Kyoto University, Yoshida, 606 Kyoto, Japan and Institute for Fundamental Chemistry, 34-4, Takano-Nishihiraki-cho, Sakyou-ku, 606 Kyoto, Japan

(Received 17 March 1992; accepted 24 July 1992)

The moderately large-embedded-cluster (MLEC) model of Grimley, Pisani, Ravenek, and others are modified so that the model is more easily applicable to *ab initio* calculations. We give a linewidth to each discrete energy level of a cluster for simulating the density of states of a bulk metal and for preventing from the singularity. The dependence of the calculated results on this linewidth is shown to be small. Symmetric orthogonalization of a basis set and a new convergence algorithm are adopted in writing up our *ab initio* program. These modifications give a rapid convergence of the density matrix in the self-consistent-field calculation. Test calculations are performed for hydrogen adsorption on a Li (100) surface with the use of several cluster and embedded cluster models.

I. INTRODUCTION

The cluster model is based on the locality of surface–molecule interactions. A large number of cluster model calculations have been performed for studying surface reactions and it is proved that the cluster model is useful for clarifying the mechanism of chemisorption and electronic structures of active sites. In previous *ab initio* calculations on small Li clusters, various adsorption sites were compared. The bridge or hole site of the Li (100) surface has been found to be most favorable, though the energy differences among the bridge, hole, and on-top sites were rather small. The cluster model does not include enough effect of the bulk solid and is not prevented from an artificial boundary effect due to a finite size of the cluster. The calculated adsorption energy depends on the cluster size. The heats of atomic hydrogen adsorption on a Li cluster are reported to vary from 5 to 70 kcal/mol for different Li clusters.[1–8]

Some models have been proposed for including the effect of bulk metal. For surface–molecule interactions in which electron transfer between surface and adsorbate is important, the dipped adcluster model is proposed from this laboratory.[9] The adcluster, which is a combined system of adsorbate and cluster, is dipped onto the electron bath of a solid surface and is made equilibrium for electron exchange. The electrostatic image force between adsorbate and surface is also taken into account. This model has been applied successfully to O_2 chemisorptions on palladium and silver surfaces.[9,10]

On the other hand, Grimley and Pisani proposed earlier the method in which the surface–adsorbate system is embedded on a surface (actually on a larger cluster) and is attempted to connect with the outer surface region. This embedded cluster model has been extended by many authors.[11–44] This model is intuitively so charming that we tried to use this model by preparing an *ab inito* program.

In this work, we adopt the moderately large-embedded-cluster (MLEC) method of Grimley *et al.* based on the Green's function method.[11–20] For *ab initio* calculations, the size of the metal cluster appearing in the model is very important; it is difficult to use a moderately large cluster for representing the solid. We therefore modify the MLEC method such that the calculational labor is reduced by modifying the Green's function method and some other computational techniques. We have coded an *ab initio* program based on the program "GAMESS."[45]

Section II gives a brief derivation of the MLEC method proposed by Pisani.[13] In Sec. III, a formalism of symmetric orthogonalization is presented instead of the orthogonalization of the basis set by Ravenek and Geurts,[20] and in Sec. IV, a new convergence algorithm is summarized. In Sec. V, we modify the Green's function method so that it is able to take into account the linewidth of the energy levels of a cluster. In Sec. VI, additional terms in the Fock matrix due to the electrostatic potential, and in Sec. VII, the behavior of the coupling matrix in the present calculations is presented. In Sec. VIII, the calculation of the hydrogen adsorption on a Li (100) surface is performed with the use of several cluster and embedded cluster models; Li_4, Li_{10}, and Li_{14} clusters; and Li_4 embedded in Li_6 and Li_{10} clusters. The calculated results and the comparison between the two models are given.

II. METHOD

We explain here the MLEC model of Pisani *et al.* which is the starting basis of the present study. The surface–adsorbate system is illustrated in Fig. 1, where the adsorbate is represented by A and the solid surface by $B \cup D$. In the cluster model, the system is represented by the cluster B interacting with the adsorbate A. In the embedded cluster model, the self-consistent-field (SCF) calculation on the $A \cup B$ region is performed considering the

 0021-9606/92/216535-09$006.00

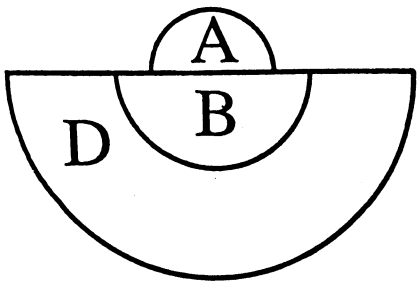

FIG. 1. A schematic representation of the embedded cluster model. A is the adsorbate, B the cluster, and D represents the solid.

effect of D. The embedding scheme is performed based on the restricted Hartree–Fock (RHF) approximation.

The Fock matrix F in the RHF–Roothaan method and its total energy E are given as a functional of the one-electron density P as

$$F(P)C=SC\varepsilon, \tag{1}$$

$$E=\sum_{\lambda\sigma} P_{\lambda\sigma}[H+F(P)]_{\lambda\sigma}, \tag{2}$$

where

$$F_{\mu\nu}=H_{\mu\nu}+\sum_{\lambda\sigma} P_{\lambda\sigma}\left[(\mu\nu|\sigma\lambda)-\frac{1}{2}(\mu\lambda|\sigma\nu)\right], \tag{3}$$

and H, S, C, and ε are core-Hamiltonian, overlap, the linear combination of atomic orbital–molecular orbital (LCAO–MO) coefficient, and orbital energy matrices, and $(\mu\nu|\sigma\lambda)$ is the electron repulsion integral.

The Green's function G and a matrix Q are defined by

$$Q(z)G(z)=1, \tag{4}$$

$$Q(z)=zS-F. \tag{5}$$

So, the Green's function G is given by

$$G(z)=(zS-F)^{-1}, \tag{6}$$

$$G_{\lambda\sigma}(z)=\sum_i \frac{C_{\lambda i}C_{\sigma i}}{z-\varepsilon_i}. \tag{7}$$

The density matrix is given as an integral of the Green's function

$$P_{\lambda\sigma}=\frac{1}{2\pi i}\oint G_{\lambda\sigma}(z)dz, \tag{8}$$

where the integral path is around the poles corresponding to the occupied orbitals.

Let the interaction between A and D be small enough to approximate

$$Q_{AD}=0,\quad Q_{DA}=0,\quad G_{AD}=0,\quad \text{and}\quad G_{DA}=0, \tag{9}$$

then Eq. (4) becomes

$$\begin{pmatrix} Q_{AA} & Q_{AB} & 0 \\ Q_{BA} & Q_{BB} & Q_{BD} \\ 0 & Q_{DB} & Q_{DD} \end{pmatrix}\begin{pmatrix} G_{AA} & G_{AB} & 0 \\ G_{BA} & G_{BB} & G_{BD} \\ 0 & G_{DB} & G_{DD} \end{pmatrix}=\begin{pmatrix} 1 & 0 & 0 \\ 0 & 1 & 0 \\ 0 & 0 & 1 \end{pmatrix}. \tag{10}$$

After a matrix manipulation, we obtain

$$\begin{pmatrix} Q_{AA} & Q_{AB} \\ Q_{BA} & Q_{BB} \end{pmatrix}\begin{pmatrix} G_{AA} & G_{AB} \\ G_{BA} & G_{BB} \end{pmatrix}=\begin{pmatrix} 1 & 0 \\ 0 & 1-Q_{BD}G_{DB} \end{pmatrix}, \tag{11}$$

in which the elements on the left-hand side belong only to the $A\cup B$ region.

Suppose that in the adsorption of A on B, the interaction between B and D is constant

$$Q_{BD}G_{DB}=Q^f_{BD}G^f_{DB}, \tag{12}$$

where the superscript f specifies the value for the free solid $B\cup D$ without the adsorbate A. Equation (11) then becomes

$$\begin{pmatrix} Q_{AA} & Q_{AB} \\ Q_{BA} & Q_{BB} \end{pmatrix}\begin{pmatrix} G_{AA} & G_{AB} \\ G_{BA} & G_{BB} \end{pmatrix}=\begin{pmatrix} 1 & 0 \\ 0 & 1-Q^f_{BD}G^f_{DB} \end{pmatrix}, \tag{13}$$

$$\begin{pmatrix} G_{AA} & G_{AB} \\ G_{BA} & G_{BB} \end{pmatrix}=\begin{pmatrix} Q_{AA} & Q_{AB} \\ Q_{BA} & Q_{BB} \end{pmatrix}^{-1}\begin{pmatrix} 1 & 0 \\ 0 & 1-Q^f_{BD}G^f_{DB} \end{pmatrix}. \tag{14}$$

We denote the inverse of the matrix Q (Q^{-1}) in Eq. (14) by $\overline{G}$,

$$\begin{pmatrix} G_{AA} & G_{AB} \\ G_{BA} & G_{BB} \end{pmatrix}=\begin{pmatrix} \overline{G_{AA}} & \overline{G_{AB}} \\ \overline{G_{BA}} & \overline{G_{BB}} \end{pmatrix}\begin{pmatrix} 1 & 0 \\ 0 & 1-Q^f_{BD}G^f_{DB} \end{pmatrix}. \tag{15}$$

We can get the density matrix with the embedding effect as follows:

(Step 1) The matrices Q^f and G^f are given by the HF calculation for the free $B\cup D$ region, and the initial value of $\overline{G}$ is given by the HF calculation for the $A\cup B$ region.

(Step 2) G is calculated from $\overline{G}$ by Eq. (15), and the density matrix P with embedding effect is given by Eq. (8).

(Step 3) The F matrix in Eq. (1) is calculated from the new density matrix P.

(Step 4) Perform steps 2 and 3 iteratively until P converges.

We adopt the scheme of Ravenek and Geurts[20] who exclude the numerical integration in Eq. (8) and give the analytic form of the density matrix P. Using Eqs. (7), (8), and (14), we obtain the analytic form of the density matrix in the RHF approximation as

$$P_{rs}=2\sum_i^{\text{occ}} C_{ri}C_{si},\quad r\in A\cup B,\ s\in A,$$

$$P_{rs}=2\sum_i^{\text{occ}} C_{ri}C_{si}+2\sum_i^{\text{occ}}\sum_a^{B} C_{ri}C_{ai}X(a,s,i)$$

$$-2\sum_i^{\text{uoc}}\sum_a^{B} C_{ri}C_{ai}X(a,s,i),\quad r\in A\cup B,\ s\in B, \tag{16}$$

$$X(a,s,i)=\begin{cases}\sum_{b}^{D}\sum_{j}^{\text{uoc}}\dfrac{C_{bj}^{f}C_{sj}^{f}(F^{f}-\varepsilon_{j}^{f}S^{f})_{ab}}{\varepsilon_{i}-\varepsilon_{j}^{f}}, & \varepsilon_{i}\in\text{occ}\\ \sum_{b}^{D}\sum_{j}^{\text{occ}}\dfrac{C_{bj}^{f}C_{sj}^{f}(F^{f}-\varepsilon_{j}^{f}S^{f})_{ab}}{\varepsilon_{i}-\varepsilon_{j}^{f}}, & \varepsilon_{i}\in\text{uoc},\end{cases} \tag{17}$$

where occ and uoc denote the occupied and unoccupied orbitals, respectively. We introduce the coupling matrix M, which is defined by

$$P_{rs}=\sum_{k}^{\text{all}}\sum_{a}^{B}C_{rk}C_{ak}M_{sa}(\varepsilon_{k}), \tag{18}$$

$$M_{sa}(\varepsilon)=\begin{cases}2\delta_{sa}+2\sum_{b}^{D}\sum_{j}^{\text{uoc}}\dfrac{C_{bj}^{f}C_{sj}^{f}(F^{f}-\varepsilon_{j}^{f}S^{f})_{ab}}{\varepsilon-\varepsilon_{j}^{f}}, & \varepsilon\leqslant\varepsilon^{f}\\ -2\sum_{b}^{D}\sum_{j}^{\text{occ}}\dfrac{C_{bj}^{f}C_{sj}^{f}(F^{f}-\varepsilon_{j}^{f}S^{f})_{ab}}{\varepsilon-\varepsilon_{j}^{f}}, & \varepsilon>\varepsilon^{f}.\end{cases} \tag{19}$$

In the cluster model, the coupling matrix elements are

$$M_{sa}(\varepsilon)=\begin{cases}2\theta(\varepsilon-\varepsilon^{f}), & \varepsilon\leqslant\varepsilon^{f}\\ 0, & \varepsilon>\varepsilon^{f},\end{cases} \tag{20}$$

where ε^{f} is a Fermi energy and θ is a step function.

III. BASIS SET

In *ab initio* calculations of the embedded cluster model, the basis set is very important since we have to divide the cluster B from the larger cluster $B\cup D$ and this division is usually defined by classifying the basis functions into those belonging to either the B or D region. The coupling matrix, e.g., depends on the basis set since the definition of the B and D regions depends on the classification of the basis set used. In the nonorthogonal basis, since there are overlaps between the basis in the B region and the one in the D region, the coupling matrix elements become large and strongly dependent on the orbital energy. This gives a difficulty in the convergence of the SCF calculation. The orthogonalization of the basis of the $B\cup D$ region improves the behavior of the coupling matrix.[20] We perform the symmetric-orthogonalization method described below which localizes each basis on each atom.

We define the overlap matrix S and the transformation matrix Q as

$$Q^{\dagger}SQ=1, \quad Q=S^{-1/2}, \tag{21}$$

$$\begin{pmatrix}Q_{BB} & Q_{BD}\\ Q_{DB} & Q_{DD}\end{pmatrix}^{\dagger}\begin{pmatrix}S_{BB} & S_{BD}\\ S_{DB} & S_{DD}\end{pmatrix}\begin{pmatrix}Q_{BB} & Q_{BD}\\ Q_{DB} & Q_{DD}\end{pmatrix}=\begin{pmatrix}1 & 0\\ 0 & 1\end{pmatrix}. \tag{22}$$

We transform the basis χ as

$$\chi'=\chi W, \quad W=\begin{pmatrix}1 & 0 & 0\\ 0 & Q_{BB} & Q_{BD}\\ 0 & Q_{DB} & Q_{DD}\end{pmatrix}. \tag{23}$$

Namely, with the matrix W, only the elements of the $B\cup D$ region in the system $A\cup B\cup D$ are orthogonalized

$$\begin{pmatrix}1 & 0 & 0\\ 0 & Q_{BB} & Q_{BD}\\ 0 & Q_{DB} & Q_{DD}\end{pmatrix}^{\dagger}\begin{pmatrix}S_{AA} & S_{AB} & 0\\ S_{BA} & S_{BB} & S_{BD}\\ 0 & S_{DB} & S_{DD}\end{pmatrix}\begin{pmatrix}1 & 0 & 0\\ 0 & Q_{BB} & Q_{BD}\\ 0 & Q_{DB} & Q_{DD}\end{pmatrix}=\begin{pmatrix}S_{AA} & S'_{AB} & S'_{AD}\\ S'_{BA} & 1 & 0\\ S'_{DA} & 0 & 1\end{pmatrix}. \tag{24}$$

Since the new basis χ'_{D} is localized on the atoms of the D region, the elements S'_{AD} and S'_{DA} should be small enough, so that we assume $S'_{AD}=0$ and $S'_{DA}=0$. Thus this transformation satisfies Eq. (9). Using Eq. (24), Eq. (17) becomes,

$$X(a,s,i)=\begin{cases}\sum_{b}^{D}\sum_{j}^{\text{uoc}}\dfrac{C_{bj}^{f}C_{sj}^{f}F_{ab}^{f}}{\varepsilon_{i}-\varepsilon_{j}^{f}}, & \varepsilon_{i}\in\text{occ}\\ \sum_{b}^{D}\sum_{j}^{\text{occ}}\dfrac{C_{bj}^{f}C_{sj}^{f}F_{ab}^{f}}{\varepsilon_{i}-\varepsilon_{j}^{f}}, & \varepsilon_{i}\in\text{uoc}.\end{cases} \tag{25}$$

IV. MODIFICATION OF THE DENSITY MATRIX CALCULATION

There are some difficulties in the SCF process of the embedded cluster model calculation.

(1) A large number of operations for calculating density matrix elements. The calculation of density matrix elements in Eq. (16) involves n^{3} operations.[20]

(2) Slow convergence in the SCF calculation. The variables for calculating the density matrix are not only the LCAO coefficients, but also their orbital energies. The increase of the variables leads to a slow convergence.

We therefore modify the algorithm of the density matrix calculation. We divide the convergence process of the LCAO coefficients from that of the orbital energies. The scheme is summarized in the following steps:

(Step 1) The matrix X in Eq. (25) is produced from C^{f}, ε^{f}, and F^{f} with ε_{i} fixed. The orbital energy ε_{i} calculated for the cluster $A\cup B$ is chosen as the initial value of ε_{i}.

(Step 2) SCF calculations are performed until P converges with fixed X. After the convergence, we get a new set of ε_{i} which are different from the old ε_{i}.

(Step 3) Replacing old ε_{i} by new ε_{i}, X in Eq. (25) is reproduced.

(Step 4) Steps 2 and 3 are done iteratively until P and ε_{i} converge.

Although the convergence depends on the initial values of P, C, and ε, the SCF cycle in step 2 costs 1/3–1/5 times the central processing unit (CPU) time for the calculation without this scheme. Without this scheme, the embedded cluster model calculation oscillated and did not show a convergence of the density matrix in the following calculations for the $Li_{n}H_{2}$ system. However, with this scheme, the embedded cluster calculations converged and several trial calculations using different initial MOs gave

the same unique stable result, i.e., the ground state. In step 2, the calculation of density matrix elements involves n^2 operations.

V. MODIFICATION OF THE GREEN'S FUNCTION

For *ab initio* calculations of surface–molecule interactions, it is usually difficult to use a large enough cluster for representing a solid surface. In a bulk metal, the conduction and the valence bands are continuous, but in the cluster model, the energy levels are discrete and there is a highest-occupied molecular orbital–lowest unoccupied molecular orbital (HOMO–LUMO) gap. Since the analytic form of the coupling matrix in Eq. (19) is different between the regions $\varepsilon<\varepsilon^f$ and $\varepsilon>\varepsilon^f$, and includes the term $1/(\varepsilon-\varepsilon_j^f)$ which is singular at $\varepsilon=\varepsilon_j^f$, the matrix elements are not smooth near the Fermi energy level. We then attempt to modify the term $1/(\varepsilon-\varepsilon_j^f)$ in order to prevent them from the singularity. We try to simulate the density of states of a bulk metal by adding a linewidth to each energy level of the cluster and modify the embedded cluster model by requiring the Green's function to consider the linewidth of each energy level. The energy gap κ,

$$\kappa=\varepsilon_{\mathrm{HOMO}}-\varepsilon_{\mathrm{LUMO}} \tag{26}$$

in the bulk metal should be zero, but is actually nonzero because of a finite size of the cluster $B\cup D$. We therefore modify the density of states so that the value is nonzero in the neighborhood of the Fermi level.

The density matrix in Eq. (8) can be written by using the δ function as

$$P_{\lambda\sigma}=\int_{-\infty}^{\varepsilon^f} d\varepsilon \sum_n^{\mathrm{all}} C_{\lambda n}C_{\sigma n}\delta(\varepsilon-\varepsilon_n), \tag{27}$$

and the δ function is rewritten as below by using the Lorentz type function

$$\begin{aligned}\delta(z-\varepsilon_n)&=\lim_{\kappa\to 0}\frac{1}{\pi}\frac{\kappa}{(z-\varepsilon_n)^2+\kappa^2}\\&=\lim_{\kappa\to 0}\frac{1}{\pi}\mathrm{Im}\left(\frac{\kappa}{z-\varepsilon_n+i\kappa}\right),\end{aligned} \tag{28}$$

where i is the imaginary unit. We put Eq. (28) into Eq. (27) and obtain

$$\begin{aligned}P_{\lambda\sigma}&=\lim_{\kappa\to 0}\frac{1}{\pi}\int_{-\infty}^{\varepsilon^f} dz\,\mathrm{Im}\sum_n\left(\frac{C_{\lambda n}C_{\sigma n}}{z-\varepsilon_n+i\kappa}\right)\\&=\lim_{\kappa\to 0}\mathrm{Re}\left(\frac{1}{2\pi i}\oint dz\sum_n\frac{C_{\lambda n}C_{\sigma n}}{z-\varepsilon_n+i\kappa}\right),\end{aligned} \tag{29}$$

where the integral path is taken around the poles corresponding to the occupied orbitals.

Let each orbital energy have a Lorentz type distribution whose half value is equal to κ',

$$\kappa'=\frac{\varepsilon_{\mathrm{HOMO}}-\varepsilon_{\mathrm{LUMO}}}{2}, \tag{30}$$

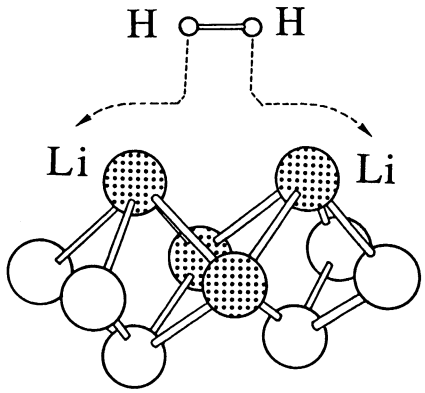

FIG. 2. A Li_{10} cluster interacting with H_2. The four shaded Li atoms compose the B region and the other Li atoms the D region, and H_2 is the adsorbate A in Fig. 1.

then the density of states for the cluster $B\cup D$ has no energy gap. We put $\kappa=\kappa'$ instead of $\kappa\to 0$ in Eq. (29). From a comparison of Eqs. (8) and (29), the Green's function is written as

$$G_{\lambda\sigma}(z)=\mathrm{Re}\left(\sum_n\frac{C_{\lambda n}C_{\sigma n}}{z-\varepsilon_n+i\kappa}\right). \tag{31}$$

Using Eq. (31) instead of Eq. (7), we get the density matrix as

$$\begin{aligned}P_{rs}&=\sum_i^{\mathrm{occ}} C_{ri}C_{si},\quad r\in A\cup B,\ s\in A,\\P_{rs}&=\sum_i^{\mathrm{occ}} C_{ri}C_{si}+\sum_i^{\mathrm{occ}}\sum_a^{B} C_{ri}C_{ai}X(a,s,i)\\&\quad-\sum_i^{\mathrm{uoc}}\sum_a^{B} C_{ri}C_{ai}X(a,s,i),\quad r\in A\cup B,\ s\in B,\end{aligned} \tag{32}$$

where

$$X(a,s,i)=\begin{cases}\displaystyle\sum_b^{D}\sum_j^{\mathrm{uoc}}\frac{C_{bj}^f C_{sj}^f F_{ab}^f}{\varepsilon_i-\varepsilon_j^f+[\kappa^2/(\varepsilon_i-\varepsilon_j^f)]}, & \varepsilon_i\in\mathrm{occ}\\ \displaystyle\sum_b^{D}\sum_j^{\mathrm{occ}}\frac{C_{bj}^f C_{sj}^f F_{ab}^f}{\varepsilon_i-\varepsilon_j^f+[\kappa^2/(\varepsilon_i-\varepsilon_j^f)]}, & \varepsilon_i\in\mathrm{uoc}.\end{cases} \tag{33}$$

If the cluster is large enough, then $\kappa'\to 0$ and the modified Green's function becomes equivalent to the original one, or else the density matrix and the electronic energy depend on the value of κ'.

We examine the κ' dependence for the adsorption energy. The Li crystal has a body-centered-cubic lattice with the lattice constant of 3.52 Å. We use a Li_{10} cluster shown in Fig. 2 as the large cluster $B\cup D$ which is supposed to represent the Li (100) surface. The shaded four atoms represent the B region and the others represent the D region. For the Li atom, STO-3G basis plus diffuse s function ($\zeta=0.076$) is used.[6]

We set the Fermi energy ε^f and κ' as

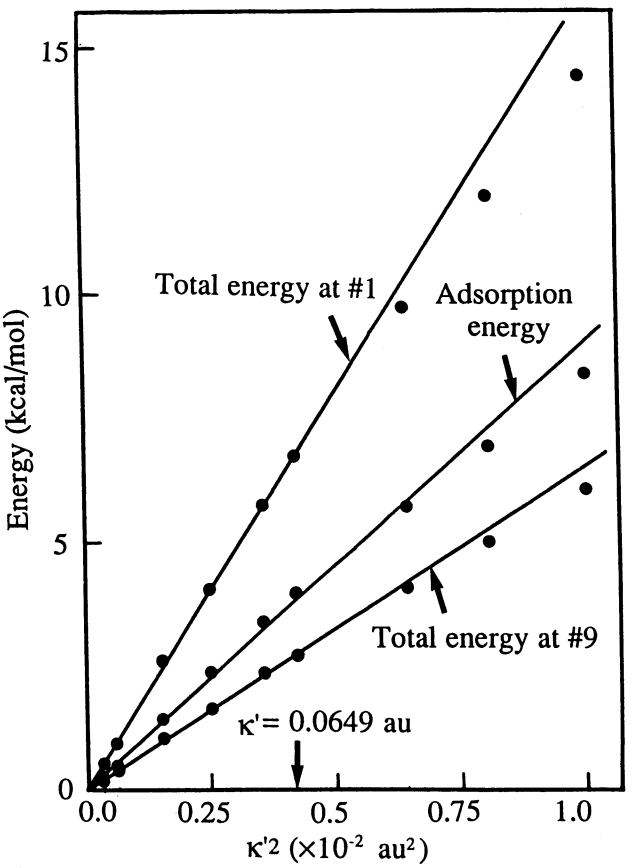

FIG. 3. κ' dependence of total and adsorption energies. The energies are plotted vs κ'^2. Each value for $\kappa'=0$ is taken to be zero.

$$\varepsilon^f=\frac{\varepsilon_{\mathrm{HOMO}}+\varepsilon_{\mathrm{LUMO}}}{2}=-0.027 \text{ a.u.}, \tag{34}$$

$$\kappa'=\frac{\varepsilon_{\mathrm{LUMO}}-\varepsilon_{\mathrm{HOMO}}}{2}=0.0649 \text{ a.u.}, \tag{35}$$

where the values of $\varepsilon_{\mathrm{HOMO}}$ and $\varepsilon_{\mathrm{LUMO}}$ are due to the Li_{10} cluster calculation.

Figure 3 shows the κ' dependence of the total and adsorption energies for Li_4 embedded in the Li_6 cluster model. Since Eq. (33) depends on not κ', but κ'^2, the energies are plotted against κ'^2 in the range of $0.02\leqslant\kappa'\leqslant0.1$ a.u. If the value of κ' is less than 0.02 a.u., the embedded cluster model did not show convergence and the total energy was not obtained. The extrapolation of the energies for several values of κ' gives the energies for $\kappa'=0$ that are taken to be the origin of Fig. 3. The points "1" and "9" in Fig. 3 correspond to the free H_2+Li_{10} and on-top adsorbed H_2Li_{10} systems, respectively (the explicit coordinates are given in Table I). The total energy at points 1 and 9 for $\kappa'=0$ are -29.7919 and -29.8416 a.u., respectively, and the energy difference gives the adsorption energy for $\kappa'=0$, i.e., 31.2 kcal/mol. The adsorption energy for $\kappa'=0.0649$ a.u. defined in the same way is 34.9 kcal/mol. The difference 3.92 kcal/mol is the effect of modifying the Green's function, but is small in comparison with the absolute value of the adsorption energy.

TABLE I. Geometries of the points 1–15 along the reaction path shown in Fig. 8.[a]

Position	Distance (Å)	
	R_{H-H}	R_{Li-H}[b]
1	0.7417	20.047
2	0.7417	2.4273
3	1.0	2.0600
4	1.2	1.9290
5	1.4	1.8134
6	2.0	1.7610
7	2.5	1.6705
8	3.0	1.6139
9	3.4928	1.595
10	4.0	1.595
11	4.6	1.595
12	5.4742	1.595
13	6.644	1.5952
14	7.208	2.0147
15	7.3	1.9815

[a]The reaction path keeps the C_{2v} symmetry.
[b]Distance to the nearest Li atom.

VI. ADDITIONAL TERM IN THE FOCK MATRIX

The bulk effect on the B region is not represented by the correction of the density matrix alone. Ravenek and Geurts[20] suggested that there is an electrostatic contribution due to the charge distribution in D and that is included in the H matrix in Eq. (3). We adopt their correction and the field is estimated with the use of the population analysis. We calculate the Löwdin population for the free $B\cup D$ region without A, and replace the atoms in D by the point charges. We use the H matrix of the $A\cup B$ region with the point charges in the D region. In the following calculations, this correction is not important since the atomic populations in the D region are -0.06–$+0.15$, which are not so large.

VII. BEHAVIOR OF THE COUPLING MATRIX

We compare the coupling matrices using the nonorthogonal and semiorthogonal basis and the modified Green's function. We use the same model as shown in Fig. 2. In the cluster model, the coupling matrix M is given by Eq. (20).

Some elements of the coupling matrix by the nonorthogonal basis are shown in Fig. 4. The diagonal and off-diagonal elements show an energy dependence and the off-diagonal element is quite large. The corresponding coupling matrix elements obtained by the semiorthogonal basis are shown in Fig. 5. The diagonal elements show a step-function shape and the off-diagonal element is small, but around the Fermi energy level, they show a sharp maximum or minimum. The effect of the orthogonalization on the coupling matrix is reported previously by Ravenek and Geurts.[20]

Figure 6 shows the corresponding coupling matrix elements calculated by the semiorthogonal basis and with the modified Green's function explained above. The diagonal elements look like step functions and the off-diagonal

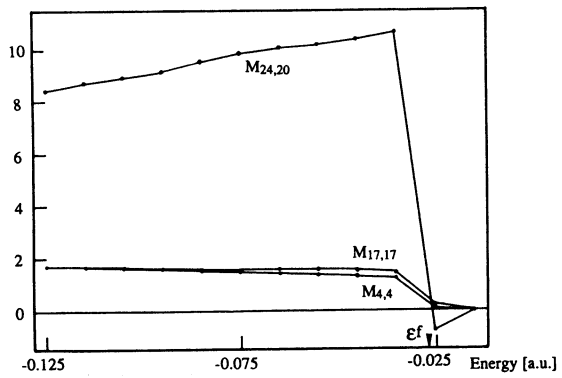

FIG. 4. Coupling matrix elements for the nonorthogonal basis.

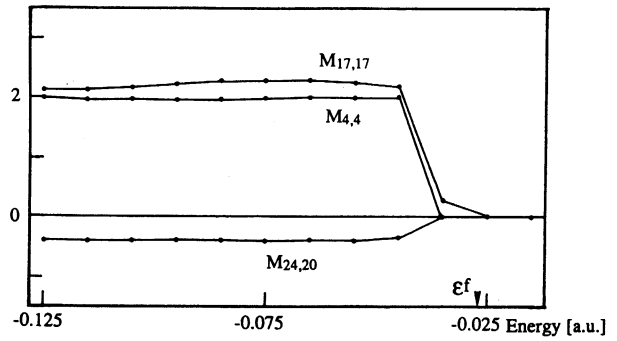

FIG. 6. Coupling matrix elements for the semiorthogonal basis with modified Green's function.

element is very small for all the values of energy. The maximum and the minimum near the Fermi energy level disappear. This result indicates an easy convergence of the density in the SCF calculations. We therefore adopt Eqs. (32) and (33) using the semiorthogonal basis and the modified Green's function in the following calculations.

VIII. CALCULATION OF H_2 ADSORPTION ON A Li SURFACE

The embedded cluster model has been applied to the adsorption of a H_2 molecule on a Li (100) surface. Ravenek and Geurts[20] studied the Li–H system using the embedded cluster model.

We use the Li_{10} and Li_{14} clusters shown in Figs. 2 and 7, respectively, as the $B \cup D$ region. The shaded four atoms represent the B region and the others the D region. The clusters are supposed to represent the Li (100) surface and to hold the bulk lattice structure throughout the hydrogen-adsorption processes. The H_2 molecule is assumed to approach horizontally and interacts mainly with the shaded atoms. The Gaussian basis set for the Li atom is the same as the one used in the previous section, and for the H atom, the double zeta (4-31G) set is used.

We perform five different calculations for the cluster and embedded cluster calculations in order to clarify the embedding effect; they are the Li_4 cluster, Li_4 embedded in Li_6 and Li_{10} clusters giving, respectively, Li_{10} and Li_{14} $B \cup D$ clusters, and Li_{10} and Li_{14} full-cluster models. The two embedded cluster calculations are thought to have simulated, respectively, the last two cluster calculations. These five calculations are performed on the same reaction path shown in Fig. 8. Several coordinates along the reaction path are shown in Table I. At points 1 and 2, the H–H distance is kept at the equilibrium bond length of a free H_2 molecule. From points 7 to 10, the Li_2–H_2 distance is kept to 1.595 Å, which is the Li–H equilibrium distance for the on-top adsorption. From points 10 to 12, the Li–H distance is kept at 1.595 Å. In order to satisfy the condition of Eq. (9) for the embedded cluster model, the hydrogen is moved, keeping the direct interaction with the Li atoms in the D region as small as possible. The distance from points 9 to 12 is only 0.2536 Å, which is small in comparison with the Li–Li distance 3.4928 Å. Beyond point 12, the present embedded model calculation is limited because there the direct interaction between A and D is not negligible. We therefore perform only cluster model calculations in this region.

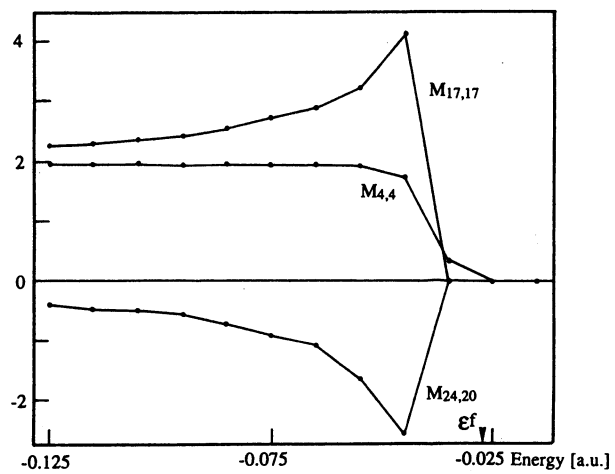

FIG. 5. Coupling matrix elements for the semiorthogonal basis.

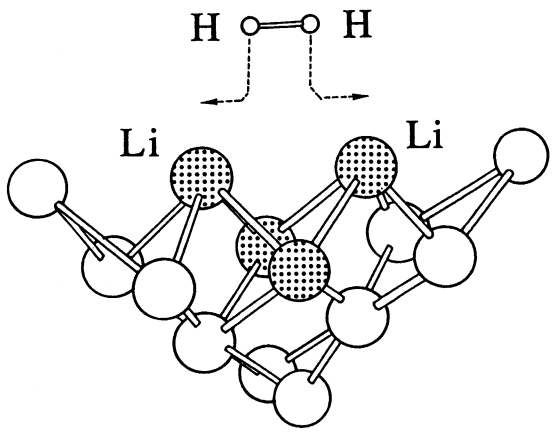

FIG. 7. A Li_{14} cluster interacting with H_2. The four shaded Li atoms compose the B region and the other Li atoms the D region, and H_2 is the adsorbate A in Fig. 1.

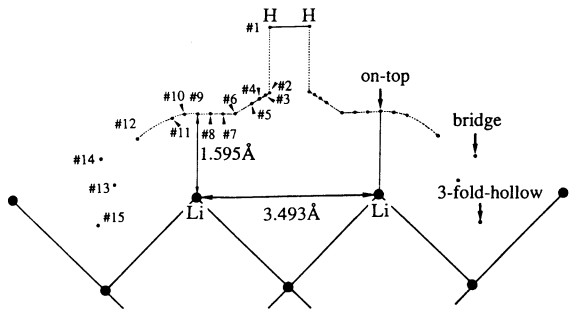

FIG. 8. The reaction path for the H_2 adsorption on a Li surface. This reaction path keeps the C_{2v} symmetry and is the same for all of the five different cluster and embedded cluster calculations, except that some Li atoms are missing in some models. Points 13, 14, and 15 are the most stable structures for the Li_4H_2, $Li_{14}H_2$, and $Li_{10}H_2$ cluster models, respectively.

The potential energy curves along the reaction path are shown in Fig. 9. The results are summarized in Table II. The energy at point 1 is chosen as a standard, namely to be zero. The solid, broken, and dotted lines represent the results of the embedded cluster model calculations, Li_{10} and Li_{14} cluster model calculations, and Li_4 cluster model calculations, respectively.

By embedding the Li_4 cluster onto the larger cluster, the curve for the Li_4 cluster model is shifted up to those for the Li_4 embedded cluster models. This is reasonable in comparison with the curves obtained by the full-cluster model calculations. The value and the position of the energy barrier in the cluster model are strongly dependent on the cluster size, but in the embedded model they are less dependent on the size of the D region. The energy difference between the two embedded cluster models are less than 10 kcal/mol all over the reaction path and their potential curves are similar. The embedded cluster models give the sharp barrier of the height of 98–101 kcal/mol at point 5 and the local minimum corresponding to the on-top adsorption at point 9. The energy barrier calculated by the cluster model is 40.0 kcal/mol for Li_4, 84.8 kcal/mol for Li_{10}, and 72.3 kcal/mol for Li_{14}. The cluster models do not give the minimum in the reaction path from points 1 to 12.

The embedded cluster calculations using Li_4 as B and Li_{10} as D as shown in Fig. 6 may be considered to have to simulate the Li_{14} cluster model calculations since Li_{14} is the full $B \cup D$ cluster. The barrier of the embedded model is higher than that of the full cluster model, since the approximation of the fixed electronic effect of D on B in the embedded model cannot describe fully the relaxation of the system in the full cluster model. The potential curves for the embedded and full cluster models are also different after the barrier; the latter monotonously stabilizes up to point 12 in Fig. 8, but the former shows a minimum near the point 9 geometry, though it is less stable than the separated system by 24.7 kcal/mol. This minimum may be artificial because after point 9 geometry, the direct interaction of hydrogen with the Li atoms in the D region would occur, but poorly described in the embedded model. In other words, the Li_4 embedded cluster is too small in the

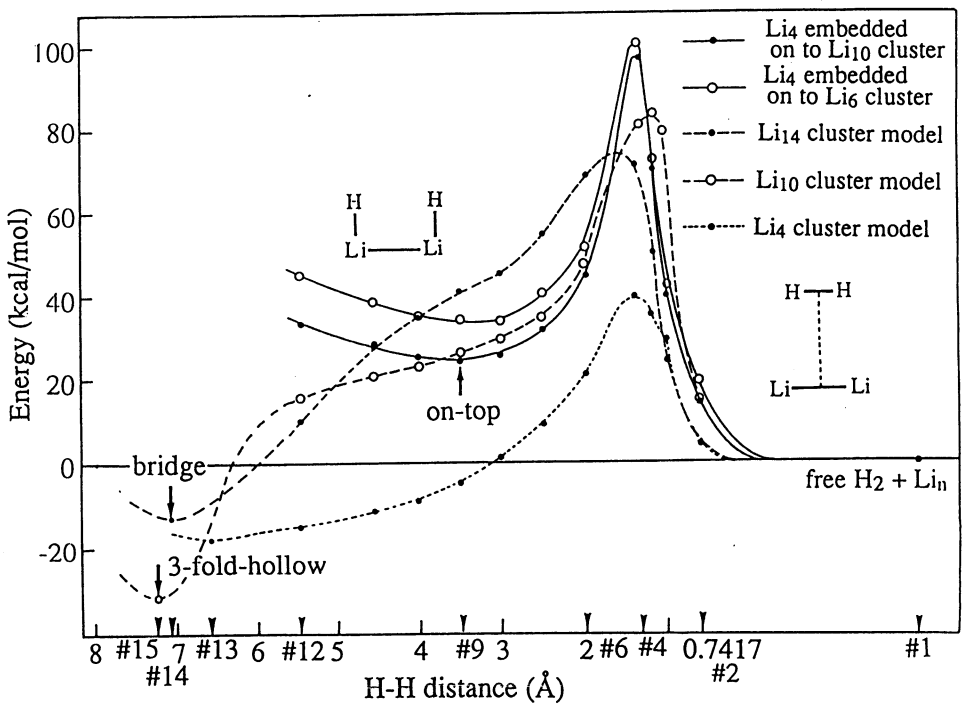

FIG. 9. Potential curves for the H_2 adsorption on a Li surface. The solid line represents the embedded cluster model, the broken and dotted line the cluster model. The most stable geometries for the cluster models which are point 13–15 geometries are shown in Fig. 10.

TABLE II. Adsorption site, adsorption barrier, adsorption energy, and atomic population of the adsorbed H for the most stable adsorption geometry calculated by the cluster and embedded cluster models.

Cluster	Adsorption site	Adsorption barrier (kcal/mol)	Adsorption energy (kcal/mol)	Atomic population on H
Li_4 cluster	On top	40.0	18.9	1.25
Li_{10} cluster	Three fold hollow	84.8	31.2	1.23
Li_{14} cluster	Bridge	72.3	14.2	1.22
Li_4 embedded onto Li_{10}	On top	98.2	−24.7	1.29
Li_4 embedded onto Li_6	On top	100.8	−34.9	1.28

region $R >$ point 9. We note that the energy for Li_4 embedded on the Li_{10} cluster is always lower than that for Li_4 embedded on Li_6.

Figure 10 shows the equilibrium geometry of the H atoms optimized for the cluster model on the Cs symmetry plane. It also shows the gross charges on each hydrogen atom. In the Li_4 cluster, a single Li–H bond is formed with the terminal Li atom. The stabilization energy relative to the free Li_4+H_2 system is 18.9 kcal/mol as shown in Fig. 10. The Li_{10} cluster adsorbs the hydrogen atom at the threefold hollow site and each hydrogen atom makes equivalent three Li–H bonds with Li_3 on the corner. The heat of adsorption is calculated to be 31.2 kcal/mol. The

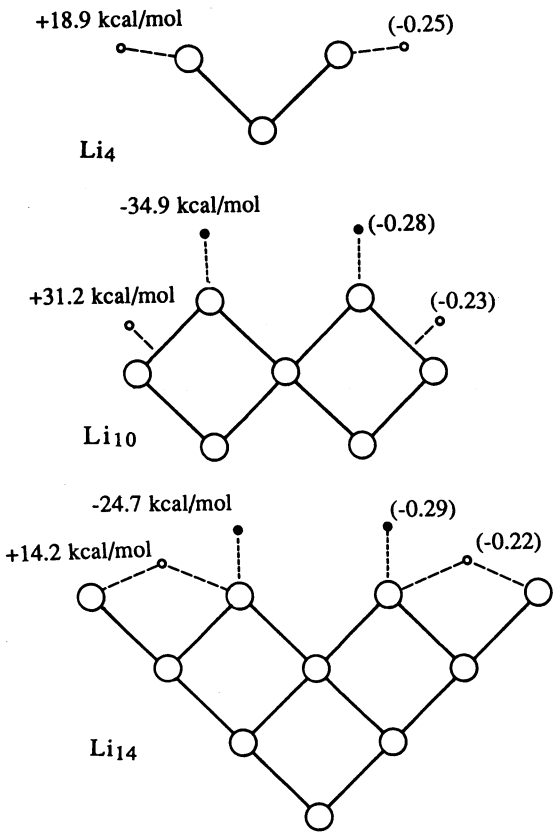

FIG. 10. Adsorption site, adsorption energy (stabilization energy relative to Li_n+H_2 in kcal/mol), and atomic population of the adsorbed hydrogen. Filled small circles represent the results of the embedded cluster model and open small circles represent the results of the cluster model. Atomic populations are shown in the parentheses.

Li_{14} cluster adsorbs the hydrogen atom at the bridge site and each hydrogen makes equivalent two Li–H bonds. The heat of adsorption for this adsorption site is calculated to be 14.2 kcal/mol, which is smaller than the adsorption energy on the threefold hollow site. These results on the adsorption site and the adsorption energy obtained for the cluster model are different from those obtained from the embedded cluster model; on-top adsorption with negative adsorption energy (−34.9 or −24.7 kcal/mol) are shown in Fig. 10. We note that this difference is due mainly to the smallness of the B region (only Li_4) in the present embedded cluster model calculation: it cannot represent the Li–H bonds in the bridge and threefold hollow sites. However, we further note that even the Li_4 cluster gives positive adsorption energy in the region $R >$ point 8: at the on-top site of point 9, it is +9.0 kcal/mol. This is in contrast to the result of the present embedded cluster model calculation.

The atomic charges of the adsorbed hydrogen are −0.25, −0.23, and −0.22 for the Li_4, Li_{10}, and Li_{14} cluster models, respectively. Those of the embedded cluster models are −0.28 and −0.29 for Li_4 on Li_6 and Li_{10}, respectively.

IX. CONCLUDING REMARKS

We have modified here the moderately large embedded cluster (MLEC) model of Grimley *et al.* and applied it to H_2 adsorption on a lithium surface. We have improved the convergence behavior of the MLEC method by giving a linewidth to each discrete energy level. The symmetric orthogonalization of basis set and the new convergence algorithm are adopted. The use of semiorthogonal basis and improved Green's function make the coupling matrix smooth and the convergence of SCF procedure easy.

The calculations of hydrogen adsorption on Li (100) surface are performed by the use of several cluster models and embedded cluster models. In the embedded cluster model, the equilibrium structure of the adsorbed hydrogen is obtained at the on-top position, but this adsorption structure is 24.7 or 34.9 kcal/mol less stable than the isolated system. In the region that the direct interaction between A and D is small, the embedded model simulates rather well the full cluster model (i.e., the $A \cup B \cup D$ model). However, outside the region, the embedded cluster model does not simulate the full cluster model well. A reason is clearly that the present MLEC model calculations are too small for dealing with the D region as a small

perturbation to the $A+B$ region. The cluster models, on the other hand, show the threefold hollow or bridge site adsorptions which are 14.2 and 31.2 kcal/mol more stable than the isolated system.

The criticism of the present result is rather difficult. If the results of the embedded cluster model should reproduce those of the full-cluster model, the results shown in Fig. 9 are by no means favorable to the embedded cluster model. On the other hand, if the D region of the embedded cluster model should be considered as representing a boundary of the bulk metal instead of an outer part of the larger cluster, the present result shown in Fig. 9 is difficult to evaluate since there is no experimental estimation on the potential surface for the dissociative adsorption of H_2 on a Li surface, especially between points 1 and 9.

For doing the embedded cluster model calculations, we have to calculate the $B \cup D$ cluster, which is Li_{10} or Li_{14} in the present calculations. For studying catalytic activity of a metal surface, we have to deal with transition metals, and doing *ab initio* calculations for even an M_n cluster ($n=10$–20) is still a very hard job. Therefore, though the calculational labor has been made somewhat smaller by the present modification of the MLEC model, a full application of this model to the transition metal surface is still difficult at present. Further, accounts of electron correlations are very important for dealing with such systems.[10]

ACKNOWLEDGMENTS

The calculations have been carried out with a FACOM M-780 computer at the Data Processing Center of Kyoto University and an HITAC M-680H computer at the Institute for Molecular Science. The authors thank the IMS Computer Center for the grants of computing time. Part of this study has been supported by a Grant-in-Aid for Scientific Research from the Japanese Ministry of Education, Science, and Culture.

[1] H. O. Beckmann and J. Koutecky, Surf. Sci. **120**, 127 (1982).
[2] G. Pacchioni, J. Koutecky, and H. O. Beckmann, Surf. Sci. **144**, 602 (1982).
[3] K. Przybylski, J. Koutecky, V. B. Koutecky, P. von Rague-Schleyer, and M. F. Guest, J. Chem. Phys. **94**, 5533 (1991).
[4] D. Post and E. J. Baerends, Surf. Sci. **109**, 167 (1981).
[5] K. Hermann and P. S. Bagus, Phys. Rev. B **17**, 4082 (1978).
[6] B. K. Rao, P. Jena, and M. Mannien, Phys. Rev. Lett. **53**, 2300 (1984).
[7] A. K. Ray and A. S. Hira, Phys. Rev. B **37**, 9943 (1988).
[8] A. S. Hira and A. K. Ray, Phys. Rev. B **40**, 3507 (1989).
[9] H. Nakatsuji, J. Chem. Phys. **87**, 4995 (1987); H. Nakatsuji, H. Nakai, and Y. Fukunishi, *ibid.* **95**, 640 (1991).
[10] H. Nakatsuji and H. Nakai, Chem. Phys. Lett. **174**, 283 (1990).
[11] T. B. Grimley and C. Pisani, J. Phys. C **7**, 2831 (1974).
[12] T. B. Grimley and E. E. Mola, J. Phys. C **9**, 3437 (1976).
[13] C. Pisani, Phys. Rev. B **17**, 3143 (1978).
[14] C. Pisani, R. Dovesi, and P. Carosso, Phys. Rev. B **20**, 5345 (1979).
[15] C. Pisani and F. Ricca, Surf. Sci. **92**, 481 (1980).
[16] C. Pisani, R. Dovesi, and P. Ugliengo, Phys. Status Solidi B **116**, 249 (1983); **116**, 547 (1983).
[17] C. Pisani, R. Dovesi, R. Nada, and S. Tamiro, Surf. Sci. **216**, 489 (1989).
[18] M. Causa, R. Dovesi, C. Pisani, R. Colle, and A. Fortunelli, Phys. Rev. B **36**, 891 (1987).
[19] R. Dovesi, C. Pisani, and C. Roetti, Int. J. Quantum. Chem. **17**, 517 (1980).
[20] W. Ravenek and F. M. M. Geurts, J. Chem. Phys. **84**, 1613 (1986).
[21] O. Gunnarsen and H. Hjelmberg, Phys. Scr. **11**, 97 (1975).
[22] O. Gunnarsen, H. Hjelmberg, and B. I. Lundqvist, Surf. Sci. **63**, 348 (1977).
[23] R. Colle, A. Fortunelli, and O. Salvetti, J. Chem. Phys. **80**, 2654 (1984).
[24] R. A. van Santen and L. H. Toneman, Int. J. Quantum. Chem. Suppl. **2**, 83 (1977).
[25] J. Bernholc and S. T. Pantelides, Phys. Rev. B **18**, 1780 (1978).
[26] J. Bernholc, N. O. Lipari, and S. T. Pantelides, Phys. Rev. B **21**, 3545 (1980).
[27] J. E. Inglesfield, J. Phys. C **14**, 3795 (1981).
[28] J. E. Inglesfield and G. A. Benesh, Phys. Rev. B **37**, 6682 (1988).
[29] G. A. Baraff and M. Schluter, Phys. Rev. B **19**, 4965 (1979).
[30] G. A. Baraff, M. Schluter, and G. Allan, Phys. Rev. B **27**, 1010 (1983).
[31] G. A. Baraff and M. Schluter, J. Phys. C **19**, 4383 (1986).
[32] U. Lindefelt and A. Zunger, Phys. Rev. B **24**, 5913 (1981).
[33] A. R. Williams, P. J. Feibelman, and N. D. Lang, Phys. Rev. B **26**, 5433 (1982).
[34] J. L. Whitten and T. A. Pakkanen, Phys. Rev. B **21**, 4357 (1980).
[35] P. Cremaschi and J. L. Whitten, Phys. Rev. Lett. **46**, 1242 (1981).
[36] P. Cremaschi and J. L. Whitten, Surf. Sci. **112**, 343 (1981); **149**, 273 (1985).
[37] P. Cremaschi and J. L. Whitten, Chem. Phys. Lett. **111**, 215 (1984).
[38] P. V. Madhaven and J. L. Whitten, Surf. Sci. **112**, 38 (1981).
[39] P. V. Madhaven and J. L. Whitten, J. Chem. Phys. **77**, 2673 (1982).
[40] C. R. Fischer and J. L. Whitten, Phys. Rev. Lett. **49**, 344 (1982).
[41] C. R. Fischer and J. L. Whitten, Phys. Rev. B **30**, 6821 (1984).
[42] J. P. Muscat and D. M. Newns, Surf. Sci. **89**, 282 (1979); **105**, 570 (1981).
[43] J. P. Muscat and D. M. Newns, Phys. Rev. B **27**, 2025 (1979).
[44] J. P. Muscat, Surf. Sci. **99**, 609 (1980); **110**, 85 (1981); **110**, 389 (1981); **118**, 321 (1982); **148**, 237 (1984).
[45] B. R. Brooks, P. Saxe, W. D. Laidig, and M. Dupuis, Program Library No. 481, Computer Center of the Institute for Molecular Science, 1981.